

LETTER TO THE EDITOR

# Detection of protonated formaldehyde in the prestellar core L1689B<sup>★</sup>

A. Bacmann<sup>1,2</sup>, E. García-García<sup>1,2</sup>, and A. Faure<sup>1,2</sup>

<sup>1</sup> Univ. Grenoble Alpes, IPAG, F-38000 Grenoble, France

<sup>2</sup> CNRS, IPAG, F-38000 Grenoble, France

e-mail: aurore.bacmann@univ-grenoble-alpes.fr

Received September 15, 1996; accepted March 16, 1997

## ABSTRACT

Complex organic molecules (COMs) are detected in many regions of the interstellar medium, including prestellar cores. However, their formation mechanisms in cold ( $\sim 10$  K) cores remain to this date poorly understood. The formyl radical HCO is an important candidate precursor for several O-bearing terrestrial COMs in cores, as an abundant building block of many of these molecules. Several chemical routes have been proposed to account for its formation, both on grain surfaces, as an incompletely hydrogenated product of H addition to frozen-out CO molecules, or in the gas phase, either the product of the reaction between H<sub>2</sub>CO and a radical, or as a product of dissociative recombination of protonated formaldehyde H<sub>2</sub>COH<sup>+</sup>. The detection and abundance determination of H<sub>2</sub>COH<sup>+</sup>, if present, could provide clues as to whether this latter scenario might apply. We searched for protonated formaldehyde H<sub>2</sub>COH<sup>+</sup> in the prestellar core L1689B using the IRAM 30 m telescope. The H<sub>2</sub>COH<sup>+</sup> ion is unambiguously detected, for the first time in a cold ( $\sim 10$  K) source. The derived abundance agrees with a scenario in which the formation of H<sub>2</sub>COH<sup>+</sup> results from the protonation of formaldehyde. We use this abundance value to constrain the branching ratio of the dissociative recombination of H<sub>2</sub>COH<sup>+</sup> towards the HCO channel to  $\sim 10$ -30%. This value could however be smaller if HCO can be efficiently formed from gas-phase neutral-neutral reactions, and we stress the need for laboratory measurements of the rate constants of these reactions at 10 K. Given the experimental difficulties in measuring branching ratios experimentally, observations can bring valuable constraints on these values, and provide a useful input for chemical networks.

**Key words.** astrochemistry – ISM: abundances – ISM: molecules

## 1. Introduction

Despite their low temperatures, prestellar cores harbour a wealth of chemical species. In recent years, complex organic molecules (hereafter COMs), which were previously thought to trace mainly warm gas in star forming regions have been detected in prestellar sources (e.g. Bacmann et al. 2012; Vastel et al. 2014) where the temperatures are around 10 K. The formation mechanisms of the terrestrial COMs (i.e. which are stable under Earth-like conditions) currently detected in the cold gas remain poorly understood, and the respective roles of gas-phase reactions or grain surface chemistry are debated.

Radicals like the formyl radical HCO or the methoxy radical CH<sub>3</sub>O have drawn attention as the possible precursors of COMs, either in the gas-phase (Vasyunin & Herbst 2013; Balucani et al. 2015) or on grain surfaces (Garrod & Herbst 2006). They are also important intermediates in the grain-surface synthesis of methanol, as products of H-atom additions to CO (e.g. Brown et al. 1988; Pirim & Krim 2011). These radicals are also widely detected in the gas phase of prestellar cores and cold clouds (Bacmann & Faure 2016; Agúndez et al. 2015b; Gerin et al. 2009; Cernicharo et al. 2012).

In a previous survey of these radicals in a sample of prestellar cores, Bacmann & Faure (2016) proposed that the HCO abun-

dances measured in the gas-phase could be accounted for by a pure gas-phase scenario, in which HCO results from the dissociative recombination of protonated formaldehyde H<sub>2</sub>COH<sup>+</sup>. In dark clouds, H<sub>2</sub>COH<sup>+</sup> is likely the product of the protonation of H<sub>2</sub>CO, which is an abundant organic species (with abundances generally around  $10^{-10}$ - $10^{-9}$  in prestellar cores – Bacmann et al. 2003; Guzmán et al. 2011). Proton donors like, e.g. H<sub>3</sub><sup>+</sup>, or HCO<sup>+</sup>, are the most abundant ions (with abundances close to  $10^{-9}$ - $10^{-8}$ , see Aikawa et al. 2005; Flower et al. 2005, 2006). It is therefore expected that protonated formaldehyde H<sub>2</sub>COH<sup>+</sup> would easily be formed. Previous searches by Minh et al. (1993) towards Orion A and the two cold clouds L183 and TMC-1 yielded no detection, and Ohishi et al. (1996) detected H<sub>2</sub>COH<sup>+</sup> only towards SgrB2 and several hot cores, and not towards the cold sources of their sample.

In this Letter, we present the first detection of protonated formaldehyde in a cold core, and discuss its abundance in terms of the formation of the HCO radical by ion-molecule chemistry, and the possibility to constrain the branching ratio towards HCO of its dissociative recombination with electrons.

## 2. Observations and data analysis

The frequencies of the rotational transitions of H<sub>2</sub>COH<sup>+</sup> were determined by Chomiak et al. (1994) and Dore et al. (1995) and were retrieved from the CDMS spectroscopy catalogue (Müller et al. 2001; Müller et al. 2005). Line excitation is al-

<sup>★</sup> Based on observations carried out with the IRAM 30m telescope. IRAM is supported by INSU/CNRS (France), MPG (Germany), and IGN (Spain)

ways an issue in cold ( $\sim 10$  K) gas and only levels with a low energy can be populated. To search for  $\text{H}_2\text{COH}^+$ , we therefore selected transitions with upper level energies lower than  $\sim 20$  K, which could be observed in a minimum of frequency setups, and for which good atmospheric transmission did not require very dry weather conditions. The chosen three lines at 2 mm and their spectroscopic parameters are shown in Table 1, to which we added a line at 3 mm from a previous project.

The observations were carried out in January and March 2012 for the 3 mm transition and in March 2015 for the 2 mm transitions with the IRAM 30 m telescope located at Pico Veleta, Spain, towards the prestellar core L1689B. The source was selected on the grounds that its molecular lines are usually stronger than in other similar sources (Bacmann & Faure 2016). The integration coordinates were  $\alpha_{2000} = 16^{\text{h}}34^{\text{m}}48.30^{\text{s}}$  and  $\delta_{2000} = -24^{\circ}38'04.0''$ , corresponding to the peak of the millimetre dust continuum emission. We used the receivers E090 and E150 operating at 3 mm and 2 mm, respectively, which were connected to the Fourier Transform spectrometer (FTS) at a frequency resolution of  $\sim 50$  kHz (corresponding to velocity resolutions of 0.15 km/s at 102 GHz, 0.11 km/s at 130 GHz, and 0.09 km/s at 170 GHz). The weather conditions were good during the 2012 observing runs, and excellent during the March 2015 run, with precipitable water vapour of 1 mm on average and system temperatures of  $\sim 80$  K at 126–132 GHz and  $\sim 130$  K at 170 GHz. Pointing was checked every 1.5 hours on a nearby quasar and found to be within 2–3'' at 2 mm and 3–4'' at 3 mm. Focus was performed on a strong quasar at the beginning of each observing session and on Mercury after sunrise. The data were taken with the frequency switching mode with a frequency throw of 7.5 MHz. The antenna forward efficiency  $F_{\text{eff}}$  is 0.95 and 0.93 at 3 mm and 2 mm, respectively, and the main beam efficiencies  $B_{\text{eff}}$  were taken to be 0.79, 0.77, 0.76, and 0.70 at 106.1 GHz, 126.9 GHz, 132.2 GHz, and 168.4 GHz, respectively. From integrations carried out at different offsets (which will be discussed elsewhere), we find that the emission fills the main beam but is not very extended, and therefore we used the main beam temperature scale in our analysis, applying  $T_{\text{mb}} = F_{\text{eff}}/B_{\text{eff}} T_{\text{A}}^*$ . The main beam size is 24'' at 106.1 GHz, 19'' at 126.9 GHz and at 132.2 GHz, and 15'' at 168.4 GHz.

**Table 1.** Observed  $\text{H}_2\text{COH}^+$  transitions

Transition $J_{K_a K_c}$	Frequency MHz	$E_{\text{up}}$ K	$g_{\text{up}}$	$A_{\text{ul}}$ $\text{s}^{-1}$
$4_{04} - 3_{13}$	102065.86	30.4	9	$7.27 \cdot 10^{-6}$
$2_{02} - 1_{11}$	126923.38	9.1	5	$1.83 \cdot 10^{-5}$
$2_{11} - 1_{10}$	132219.70	17.5	5	$1.55 \cdot 10^{-5}$
$1_{10} - 1_{01}$	168401.14	11.1	3	$8.77 \cdot 10^{-5}$

The data were reduced using the IRAM GILDAS/CLASS<sup>1</sup> software: the individual scans were averaged together and a low-order (typically 3) polynomial was fitted to line-free regions of the spectra to subtract a baseline. The resulting spectra were then folded to recover from the effect of the frequency switching procedure.

### 3. Column density determination

Protonated formaldehyde is clearly detected, as can be seen from the spectra shown in Fig. 1. The transition at 102 GHz is however

**Table 2.** Line parameters for the observed  $\text{H}_2\text{COH}^+$  transitions. The rms is given for 50 kHz channels. The numbers between parenthesis are the 1- $\sigma$  uncertainties. The upper limit is 3- $\sigma$ .

Frequency MHz	rms mK	$T_{\text{mb}}$ mK	$\Delta\nu$ km s <sup>-1</sup>	Integrated intensity K km s <sup>-1</sup>
102065.86	3.3	–	–	< 0.0024
126923.38	6.0	116	0.45 (0.02)	0.0553 (0.0085)
132219.70	2.6	12	0.35 (0.06)	0.0043 (0.0010)
168401.14	7.6	67	0.40 (0.03)	0.0290 (0.0048)

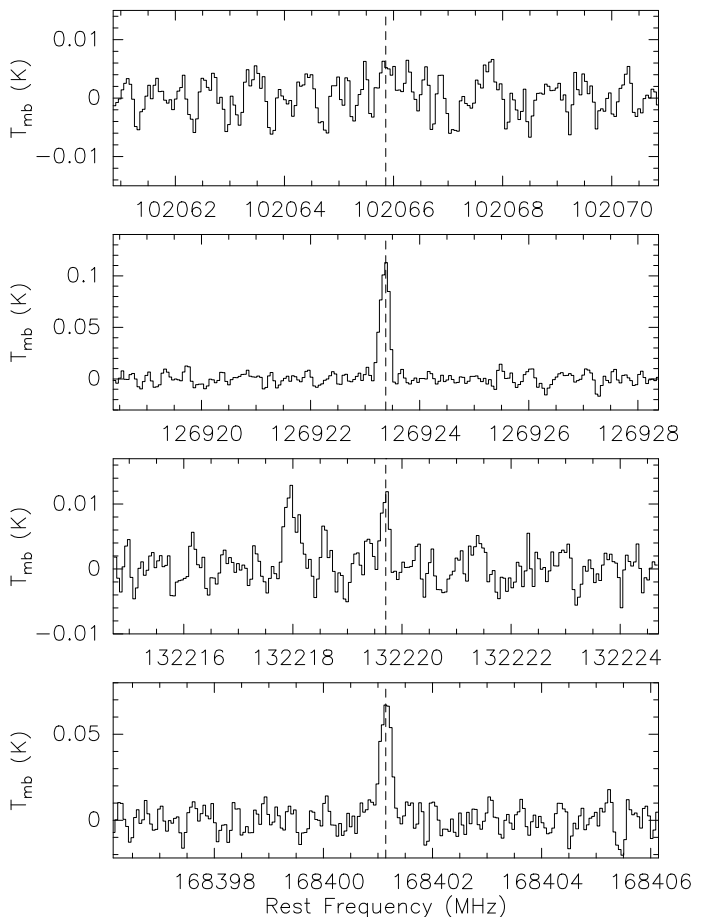


**Fig. 1.**  $\text{H}_2\text{COH}^+$  spectra in L1689B. The vertical dashed lines indicate the positions of the  $\text{H}_2\text{COH}^+$  transitions. The feature at  $\sim 132218$  MHz does not correspond to any line from the CDMS or the JPL catalogue.

not detected, which can be explained by its lower Einstein spontaneous emission coefficient and higher upper level energy. The line parameters (velocity integrated intensities, line widths, peak line intensities) were determined by fitting a Gaussian to each line. The obtained values are presented in Table 2.

There are no available collisional coefficients for  $\text{H}_2\text{COH}^+$ , so we perform a simple derivation of the column density assuming local thermodynamic equilibrium (LTE). The method we use has been described in Bacmann & Faure (2016). Briefly, we calculate the integrated intensities of the transitions under the LTE assumption for a range of column density and excitation temperature values, and perform a least-square fit, defining a  $\chi^2$  between the calculated integrated intensities and the observed integrated intensities, for the detected lines.

The best model yields a column density of  $6.7 \cdot 10^{11} \text{ cm}^{-2}$  and a temperature of 4.2 K. Reasonably good fits (i.e. for which  $\chi^2$

<sup>1</sup> <http://www.iram.fr/IRAMFR/GILDAS>

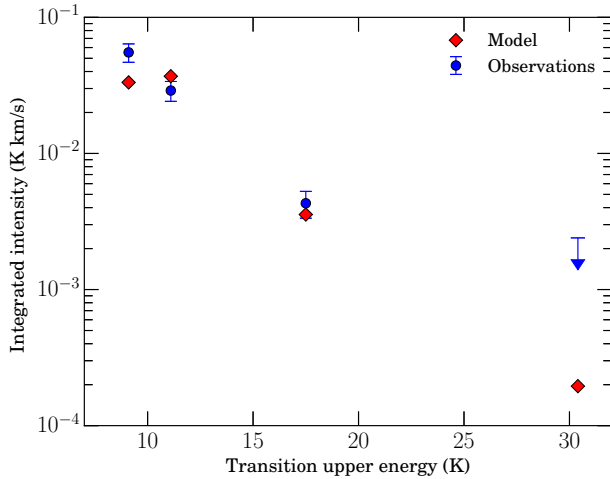


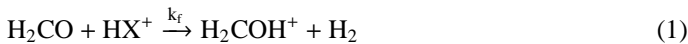
**Fig. 2.** Modelled integrated intensities compared and observed integrated intensities for the four considered  $\text{H}_2\text{COH}^+$  transitions.

is within  $1\text{-}\sigma$  of the minimum  $\chi^2$  value) can be found for high values of the column density ( $\gtrsim 1.5 \cdot 10^{12} \text{ cm}^{-2}$ ) but these are obtained for excitation temperatures which are below 3.5 K. We limit ourselves to excitation temperatures above 3.7 K because smaller values become unrealistic. With this additional condition, we find that the beam averaged  $\text{H}_2\text{COH}^+$  column density is between  $3.3 \cdot 10^{11} \text{ cm}^{-2}$  and  $1.1 \cdot 10^{12} \text{ cm}^{-2}$ . The non-detection of the 102 GHz line does not bring supplementary constraints despite the high sensitivity of the observation, because the low excitation temperatures considered ( $< 5 \text{ K}$ ) are compatible with a non-detection of this line even for unrealistically high column densities (for which the other lines would be stronger and optically thick). Despite the low number of lines in our analysis, the best fit is only moderately good, as shown in Fig.2. This probably means that the excitation deviates from LTE.

#### 4. Discussion and conclusions

This detection represents the first detection of protonated formaldehyde in a cold prestellar core. Former searches for this ion in similar sources did not yield any detection, most probably because of lack of sensitivity in the observations. The spectral resolution of the  $\text{H}_2\text{COH}^+$  non-detections in the cold sources of Ohishi et al. (1996) is ambiguous, but if we assume that it was 250 kHz, their rms noise of 20 mK was not low enough to detect the 168.4 GHz line if it was as strong as in L1689B.

Most likely, the dominant reaction route to form  $\text{H}_2\text{COH}^+$  in dark clouds is the protonation of formaldehyde



where  $\text{HX}^+$  stands for a proton donor. Indeed, both  $\text{H}_2\text{CO}$  and proton donors (like e.g.  $\text{H}_3^+$ , its deuterated isotopologues, or  $\text{HCO}^+$ ) are abundant in prestellar cores, and exothermic ion-molecule processes are generally fast. Bacmann & Faure (2016) estimated the rate for reaction (1) with  $\text{HX}^+ = \text{H}_3^+$  to be  $k_f = 7 \cdot 10^{-8} \text{ cm}^3 \text{ s}^{-1}$  at 10 K, using the locked dipole approximation. Because of the difference in reduced mass, this rate constant becomes  $k_f = 3.1 \cdot 10^{-8} \text{ cm}^3 \text{ s}^{-1}$  at 10 K if  $\text{HX}^+ = \text{HCO}^+$ . The most efficient destruction route for  $\text{H}_2\text{COH}^+$  is the dissociative recombination (DR) with electrons:



Reaction (2) was studied experimentally by Hamberg et al. (2007) (and recently by Osborne et al. 2015) who determined  $k_d = 9.9 \cdot 10^{-6} \text{ cm}^3 \text{ s}^{-1}$  at 10 K.

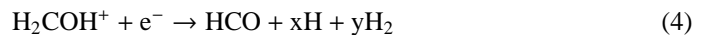
At steady state, if  $\text{H}_2\text{COH}^+$  is indeed formed mostly by reaction (1) and destroyed by reaction (2), its abundance is simply given by

$$[\text{H}_2\text{COH}^+] = \frac{k_f [\text{HX}^+]}{k_d [\text{e}^-]} [\text{H}_2\text{CO}] \quad (3)$$

Substituting the reaction rates with their values for  $\text{H}_3^+$  and assuming the proton donor abundance is equal to the electron abundance, we predict an abundance of  $[\text{H}_2\text{COH}^+] \approx 0.007 [\text{H}_2\text{CO}]$  as mentioned in Bacmann & Faure (2016), or  $[\text{H}_2\text{COH}^+] \approx 0.003 [\text{H}_2\text{CO}]$  if  $\text{HCO}^+$  is the main proton donor. Using an  $\text{H}_2\text{CO}$  column density of  $1.3 \cdot 10^{14} \text{ cm}^{-2}$  (Bacmann et al. 2003), we find that the predicted  $\text{H}_2\text{COH}^+$  column density  $N^{\text{mod}}$  derived from equation (3) is  $4.1 \cdot 10^{11} - 9.1 \cdot 10^{11} \text{ cm}^{-2}$  (depending on the main proton donor), consistent with the observed value we determine in L1689B,  $N^{\text{obs}} = 6.7 \cdot 10^{11} \text{ cm}^{-2}$  within the uncertainties. This also nicely confirms the value of the destruction rate of  $\text{H}_2\text{COH}^+$  measured by Hamberg et al. (2007) at 10 K.

Agúndez et al. (2015a) have run a time-dependent chemical model using the UMIST12 network (McElroy et al. 2013) and derive  $[\text{H}_2\text{COH}^+] \sim 8 \cdot 10^{-4} - 10^{-3} [\text{H}_2\text{CO}]$ , about six times smaller than our observed value. Though our model better reproduces the observations, it considers only one formation and one destruction route for  $\text{H}_2\text{COH}^+$ . The  $\text{H}_2\text{CO}$  protonation reactions in the UMIST12 network producing  $\text{H}_2\text{COH}^+$  have smaller reaction rates than the one we use (a factor of 2). Our model might also overestimate the amount of proton donors reacting with  $\text{H}_2\text{CO}$ , since we assume it equal to the electron abundance. We also neglect other destruction routes than electronic DR for  $\text{H}_2\text{COH}^+$ , like proton transfer between  $\text{H}_2\text{COH}^+$  and  $\text{CH}_3\text{OH}$  or  $\text{NH}_3$ , but these are about 1000 times slower than DR at 10 K and unlikely to be a cause for the discrepancy between both models.

The dissociative recombination of  $\text{H}_2\text{COH}^+$  with electrons has several output channels. According to the experiments by Hamberg et al. (2007), the products of the reaction are



where  $x$  and  $y$  are integers that account for the different possible combinations of H and  $\text{H}_2$  atoms in the products. The experimental branching ratios are 6% for  $\text{CH}_2$ , 2% for  $\text{CH}$ , and 92% for the channels where the C–O bond is conserved (i.e. CO, HCO, and  $\text{H}_2\text{CO}$ ). This is in contrast to the dissociative recombination of  $\text{CH}_3\text{OH}$  for which the C–O bond is preserved in a minority of channels (Geppert et al. 2006). In the case of  $\text{H}_2\text{COH}^+$ , the experiment by Hamberg et al. (2007) did not distinguish between HCO, CO and  $\text{H}_2\text{CO}$ .

In order to account for the gas phase abundance of the HCO radical in a sample of prestellar cores, and in particular the constant abundance ratio of  $\sim 10$  between  $\text{H}_2\text{CO}$  and HCO, Bacmann & Faure (2016) suggested that the observed HCO/ $\text{H}_2\text{CO}$  abundance ratio can be reproduced if HCO originates from the dissociative recombination of  $\text{H}_2\text{COH}^+$ , assuming that the branching ratio of the DR is  $\sim 10\%$  for the HCO channel (reaction (4) above). Although the detection of  $\text{H}_2\text{COH}^+$  in a prestellar core does not provide unambiguous evidence that

HCO does form from the protonation of formaldehyde followed by dissociative recombination, it is still in agreement with this scenario, and allows us to directly constrain the branching ratio of the dissociative recombination for the HCO channel. In this frame, and assuming the main destruction route for HCO is with a proton donor like  $\text{H}_3^+$ , the branching ratio  $f$  for HCO is given by

$$k_{\text{dd}} [\text{HCO}][\text{H}_3^+] = f k_{\text{d}} [\text{H}_2\text{COH}^+][\text{e}^-],$$

where  $k_{\text{dd}} = 5 \cdot 10^{-8} \text{ cm}^{-3} \text{ s}^{-1}$  is the destruction rate of HCO with  $\text{H}_3^+$  at 10 K (Bacmann & Faure 2016). Assuming as before  $[\text{H}_3^+] \approx [\text{e}^-]$ , the  $\text{H}_2\text{COH}^+$  column density determined in this study ( $N_{\text{H}_2\text{COH}^+}^{\text{obs}} = 6.7 \cdot 10^{11} \text{ cm}^{-2}$ ), and the HCO column density in L1689B given in Bacmann & Faure (2016) ( $N_{\text{HCO}} = 1.3 \cdot 10^{13} \text{ cm}^{-2}$ ), we find again  $f \sim 10\%$ , without invoking the  $\text{H}_2\text{CO}$  abundance.

As discussed in Bacmann & Faure (2016), another potential destruction route for HCO is with abundant atoms such as H. In this case, assuming an atomic H abundance of  $\sim 10^{-5}$  with respect to  $\text{H}_2$ , an electronic abundance of  $10^{-8}$ , and  $k_{\text{H}} = 1.5 \cdot 10^{-10} \text{ cm}^3 \text{ s}^{-1}$  for the rate constant of the reaction  $\text{HCO} + \text{H}$  (the value at 300 K from Baulch et al. 2005), we find a value for the branching ratio  $f$  of 30%. It is however unclear whether the value of  $k_{\text{H}}$  taken here also applies at 10 K, since no measurements of this rate constant are available at low temperatures.

One major uncertainty in this determination of the branching ratio results from possible alternative formation scenarios for HCO, which could be non negligible. One such route is the neutral-neutral reaction between  $\text{H}_2\text{CO}$  and an abundant radical like OH or CN. Recent experimental studies have confirmed that such reactions could proceed efficiently via tunneling at low temperatures. Indeed, Shannon et al. (2013) and Gómez Martín et al. (2014) have shown that the reaction  $\text{CH}_3\text{OH} + \text{OH}$  gets faster at low temperatures down to  $\sim 50$  K. A spectacular increase in the reaction constant is also reported by Jiménez et al. (2016) for  $\text{CH}_3\text{OCHO} + \text{OH}$  (the reaction rate increases by three orders of magnitude between 300 K and 22 K, and by an order of magnitude between 60 K and 22 K, reaching as high a value as  $1.2 \cdot 10^{-10} \text{ cm}^3 \text{ s}^{-1}$ ). In order to be as efficient as the ion-molecule route to form HCO, the constant of the reaction between  $\text{H}_2\text{CO}$  and OH would have to be  $4 \cdot 10^{-10} \text{ cm}^3 \text{ s}^{-1}$  at 10 K (Bacmann & Faure 2016). No measurements at 10 K of this reaction (or similar ones) are available, but are needed, because the behaviour of the reaction constant is not known below 230 K (at which temperature it is  $10^{-11} \text{ cm}^3 \text{ s}^{-1}$ ) and extrapolation is hazardous. In the case that  $\text{H}_2\text{CO} + \text{OH}$  would be a major formation channel for HCO, the observed HCO abundance could be accounted for without the need for the DR of  $\text{H}_2\text{COH}^+$  to yield a significant amount of HCO. In this respect, the branching ratio we determined above can be considered as an upper limit.<sup>2</sup>

This result can have implications for chemical networks because they assume statistical weights for the three products CO, HCO and  $\text{H}_2\text{CO}$  (1/3, 1/3, 1/3), as in the UMIST12 network or the KIDA<sup>3</sup> database (Wakelam et al. 2012), following Prasad & Huntress (1980). As already noted in Hamberg et al.

<sup>2</sup> We also note that the neutral-neutral reaction  $\text{CH}_2 + \text{O}$  should yield negligible amounts of HCO in the conditions prevailing in cold cores (see KIDA datasheet on this reaction). Using the rate constant in the KIDA database ( $2 \cdot 10^{-12} \text{ cm}^3 \text{ s}^{-1}$ ) and the steady-state abundances of  $\text{CH}_2$  and O from the model of Le Gal et al. (2014), we find that this reaction is 100 times less efficient than the DR of  $\text{H}_2\text{COH}^+$  at forming HCO.

<sup>3</sup> <http://kida.obs.u-bordeaux1.fr>

(2007), these branching ratios are still vastly in agreement with their experimental results which state that CO, HCO and  $\text{H}_2\text{CO}$  represent over 90% of the products. However, the branching ratio that is needed here to account for the observed HCO and  $\text{H}_2\text{COH}^+$  abundances could be significantly different from the statistical value, as it could be 10%, or lower.

This value should however be taken with some caution, because the excitation of  $\text{H}_2\text{COH}^+$  is not well constrained in the absence of collisional coefficients. Our estimation of the branching ratio should therefore be repeated once collisional coefficients for  $\text{H}_2\text{COH}^+$  become available. Observations of  $\text{H}_2\text{COH}^+$  in other prestellar sources are also needed to confirm the current findings.

To conclude, we report here the detection of protonated formaldehyde  $\text{H}_2\text{COH}^+$  in the prestellar source L1689B. The derived beam-averaged column density is  $6.7 \cdot 10^{11} \text{ cm}^{-2}$ , corresponding to an abundance of  $\sim 1.9 \cdot 10^{-11}$  with respect to  $\text{H}_2$ , if we assume an  $\text{H}_2$  column density of  $3.6 \cdot 10^{22} \text{ cm}^{-2}$  (Roy et al. 2014). This abundance is however likely overestimated, as the  $\text{H}_2$  column density in Roy et al. (2014) is averaged over a  $36''$  beam, and is probably higher in the  $15\text{--}19''$  beam of our  $\text{H}_2\text{COH}^+$  observations. The  $\text{H}_2\text{COH}^+$  column density agrees with the destruction rate of  $\text{H}_2\text{COH}^+$  by dissociative recombination as measured by Hamberg et al. (2007), supposing that  $\text{H}_2\text{COH}^+$  is mostly formed by protonation of  $\text{H}_2\text{CO}$  in prestellar cores, and destroyed by electronic dissociative recombination. Using previous observations of the radical HCO in the same source, we constrain the branching ratio of  $\text{H}_2\text{COH}^+$  to HCO to be around 10–30%, or lower if HCO is significantly formed by gas-phase reactions between  $\text{H}_2\text{CO}$  and a radical. The experimental determination of branching ratios is a fundamental piece of data in astrochemistry, but in case these measurements are not available, observations can bring valuable constraints, as demonstrated here.

*Acknowledgements.* This work has benefitted from the support of the CNRS programme "Physique et Chimie du Milieu Interstellaire" (PCMI). E. García-García acknowledges support from an Alpes Grenoble Innovation Recherche (AGIR) grant.

## References

- Agúndez, M., Cernicharo, J., de Vicente, P., et al. 2015a, A&A, 579, L10  
 Agúndez, M., Cernicharo, J., & Guélin, M. 2015b, A&A, 577, L5  
 Aikawa, Y., Herbst, E., Roberts, H., & Caselli, P. 2005, ApJ, 620, 330  
 Bacmann, A. & Faure, A. 2016, ArXiv e-prints [arXiv:1601.01696]  
 Bacmann, A., Lefloch, B., Ceccarelli, C., et al. 2003, ApJ, 585, L55  
 Bacmann, A., Taquet, V., Faure, A., Kahane, C., & Ceccarelli, C. 2012, A&A, 541, L12  
 Balucani, N., Ceccarelli, C., & Taquet, V. 2015, MNRAS, 449, L16  
 Baulch, D. L., Bowman, C. T., Cobos, C. J., et al. 2005, J. Phys. Chem. Ref. Data, 34, 757  
 Brown, P. D., Charnley, S. B., & Millar, T. J. 1988, MNRAS, 231, 409  
 Cernicharo, J., Marcelino, N., Roueff, E., et al. 2012, ApJL, 759, L43  
 Chomiak, D., Taleb-Bendiab, A., Civiš, S., & Amano, T. 1994, Can. J. Phys., 72, 1078  
 Dore, L., Cazzoli, G., Civiš, S., & Scappini, F. 1995, Chem. Phys. Lett., 244, 145  
 Flower, D. R., Pineau Des Forêts, G., & Walmsley, C. M. 2005, A&A, 436, 933  
 Flower, D. R., Pineau Des Forêts, G., & Walmsley, C. M. 2006, A&A, 449, 621  
 Garrod, R. T. & Herbst, E. 2006, A&A, 457, 927  
 Geppert, W. D., Hamberg, M., Thomas, R. D., et al. 2006, Farad. Discuss., 133, 177  
 Gerin, M., Goicoechea, J. R., Pety, J., & Hily-Blant, P. 2009, A&A, 494, 977  
 Gómez Martín, J., Caravan, R., Blitz, M., Heard, D., & Plane, J. 2014, J. Phys. Chem. A, 118, 2693  
 Guzmán, V., Pety, J., Goicoechea, J. R., Gerin, M., & Roueff, E. 2011, A&A, 534, A49  
 Hamberg, M., Geppert, W. D., Thomas, R. D., et al. 2007, Mol. Phys., 105, 899  
 Jiménez, E., Antñónolo, M., Ballesteros, B., Canosa, A., & Albaladejo, J. 2016, PCCP, 18, 2183

- Le Gal, R., Hily-Blant, P., Faure, A., et al. 2014, *A&A*, 562, 83
- McElroy, D., Walsh, C., Markwick, A. J., et al. 2013, *A&A*, 550, A36
- Minh, Y. C., Irvine, W. M., & McGonagle, D. 1993, *J. Kor. Astron. Soc.*, 26, 99
- Müller, H. S. P., Schlöder, F., Stutzki, J., & Winnewisser, G. 2005, *J. Mol. Struct.*, 742, 215
- Müller, H. S. P., Thorwirth, S., Roth, D. A., & Winnewisser, G. 2001, *A&A*, 370, L49
- Ohishi, M., Ishikawa, S.-I., Amano, T., et al. 1996, *ApJL* v.471, 471, L61
- Osborne, Jr., D. S., Lawson, P. A., & Adams, N. G. 2015, *Int. J. Mass Spectrom.*, 378, 193
- Pirim, C. & Krim, L. 2011, *Chem. Phys.*, 380, 67
- Prasad, S. S. & Huntress, Jr., W. T. 1980, *ApJS*, 43, 1
- Roy, A., André, P., Palmeirim, P., et al. 2014, *A&A*, 562, 138
- Shannon, R. J., Blitz, M. A., Goddard, A., & Heard, D. E. 2013, *Nature Chem.*, 5, 745
- Vastel, C., Ceccarelli, C., Lefloch, B., & Bachiller, R. 2014, *ApJL*, 795, L2
- Vasyunin, A. I. & Herbst, E. 2013, *ApJ*, 769, 34
- Wakelam, V., Herbst, E., Loison, J.-C., et al. 2012, *ApJS*, 199, 21